

Ro-vibrational fine structure of CF_3H by frequency-comb-assisted saturated spectroscopy at 8.6 μm

E. Vicentini¹, A. Gambetta^{1,2}, N. Coluccelli^{1,2}, E. Fasci³, A. Castrillo³, L. Gianfrani³, V. Di Sarno⁴, P. Maddaloni^{4,5}, A. Ceausu-Velcescu⁶, P. De Natale⁴, Y. Wang^{1,2}, T. T. Fernandez², P. Laporta^{1,2}, and G. Galzerano^{1,2}

¹*Dipartimento di Fisica - Politecnico di Milano, Milano, Italy*

²*Istituto di Fotonica e Nanotecnologie - CNR, Milano, Italy*

³*Dipartimento di Matematica e Fisica - Università della Campania, Caserta, Italy*

⁴*Istituto Nazionale di Ottica - CNR, Pozzuoli (NA), Italy*

⁵*INFN Istituto Nazionale di Fisica Nucleare, Sez. di Napoli, Napoli, Italy*

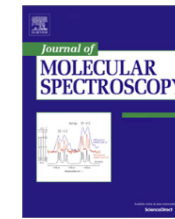
⁶*Laboratoire de Mathématiques et Physique, Université de Perpignan, France*



Contents lists available at [ScienceDirect](#)

Journal of Molecular Spectroscopy

journal homepage: www.elsevier.com/locate/jms



Assessing the time constancy of the proton-to-electron mass ratio by precision ro-vibrational spectroscopy of a cold molecular beam

L. Santamaria ^a, V. Di Sarno ^a, I. Ricciardi ^a, S. Mosca ^a, M. De Rosa ^a, G. Santambrogio ^{b,c}, P. Maddaloni ^{a,d,*}, P. De Natale ^{d,e}



Why CF_3H ?

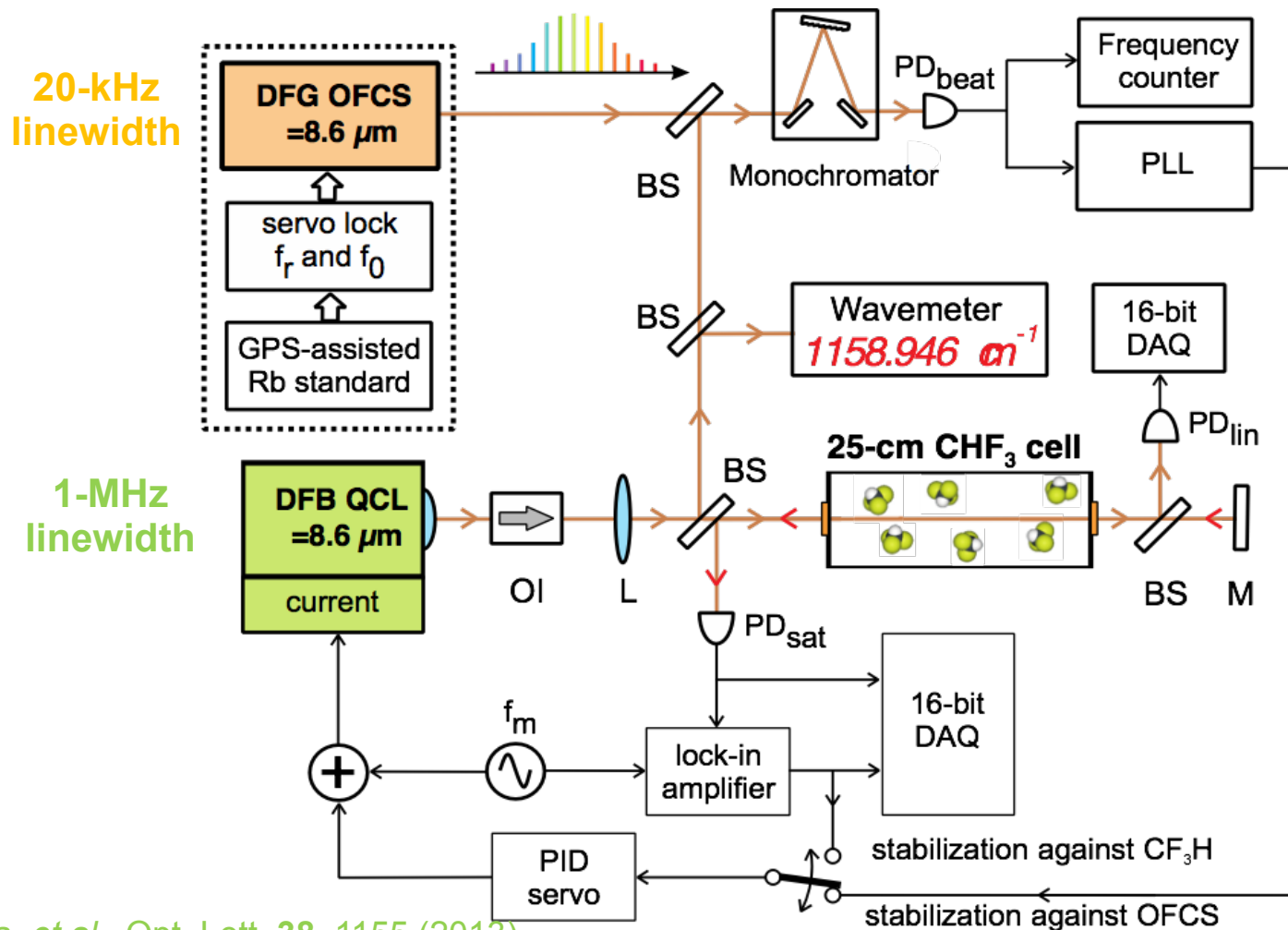
A great enhancement in the ultimate accuracy can be achieved if a **beam of slow and cold molecules** is used to implement **Ramsey-fringes technique**

CF_3H can be easily cold down in a molecular beam (buffer gas cooling and Stark manipulation) due to a high electric dipole moment

CF_3H presents favorable two-photon transition in the mid-IR

- ❑ Sub-Doppler CF_3H spectrometer at 8.6 μm
- ❑ Comb-assisted CF_3H sub-Doppler spectroscopy
- ❑ Conclusion and further activity

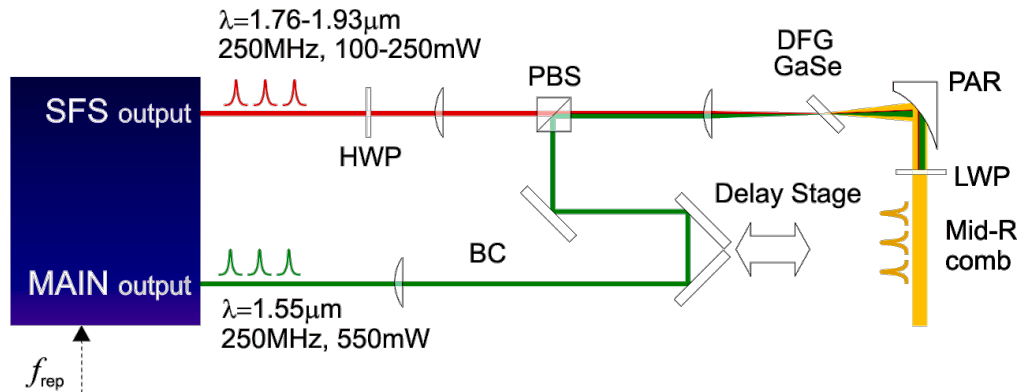
Sub-Doppler CF_3H spectrometer



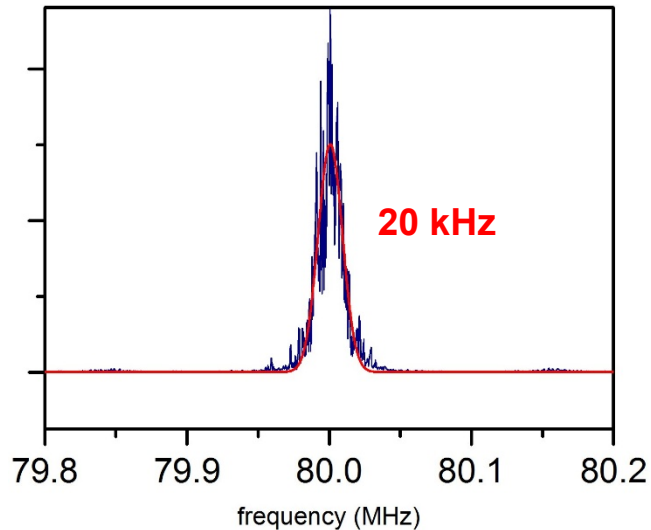
A. Gambetta, et al., Opt. Lett. 38, 1155 (2013)

E. Fasci, et al., Opt. Lett. 39, 1155 (2014)

DFG OFC at 8 – 14 μm



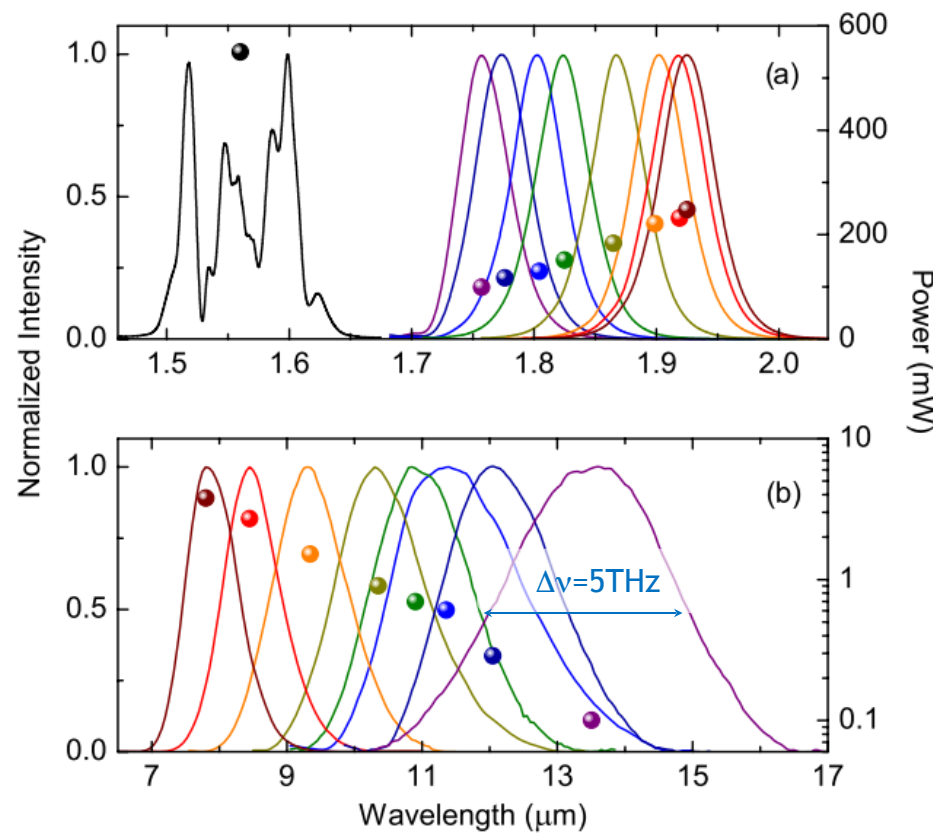
Beat with 4-kHz linewidth QCL

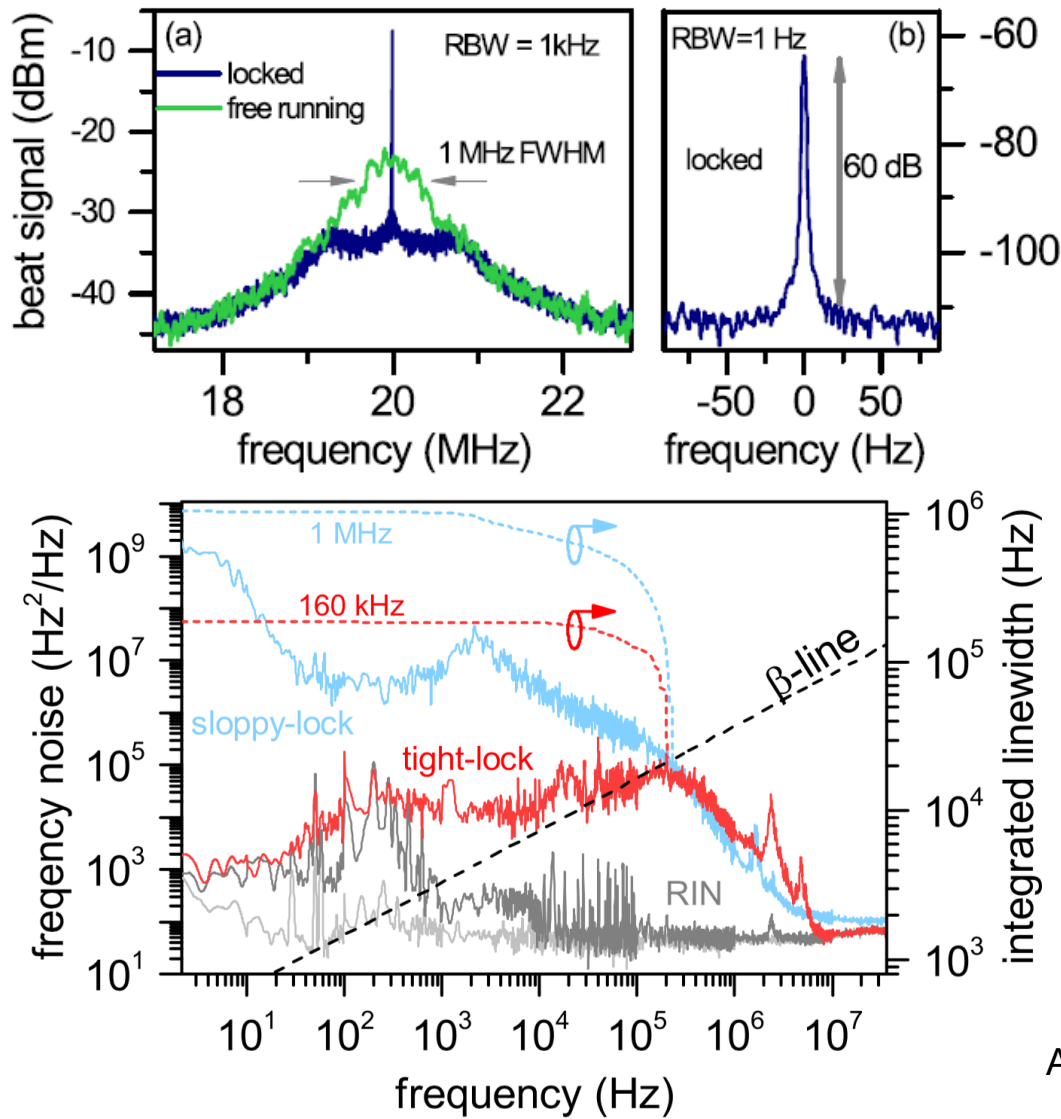


A. Gambetta, *et al.*, Opt. Lett. **38**, 1155 (2013)

GaSe CRYSTAL

High nonlinearity (50 pm/V)
Broad transparency range





Free running beatnote

Linewidth: 1 MHz

SNR: 30 dB (1-kHz RBW)

Phase-locked beatnote

Linewidth: < 1 Hz

SNR: 60 dB/Hz

54% of the RF power in the carrier

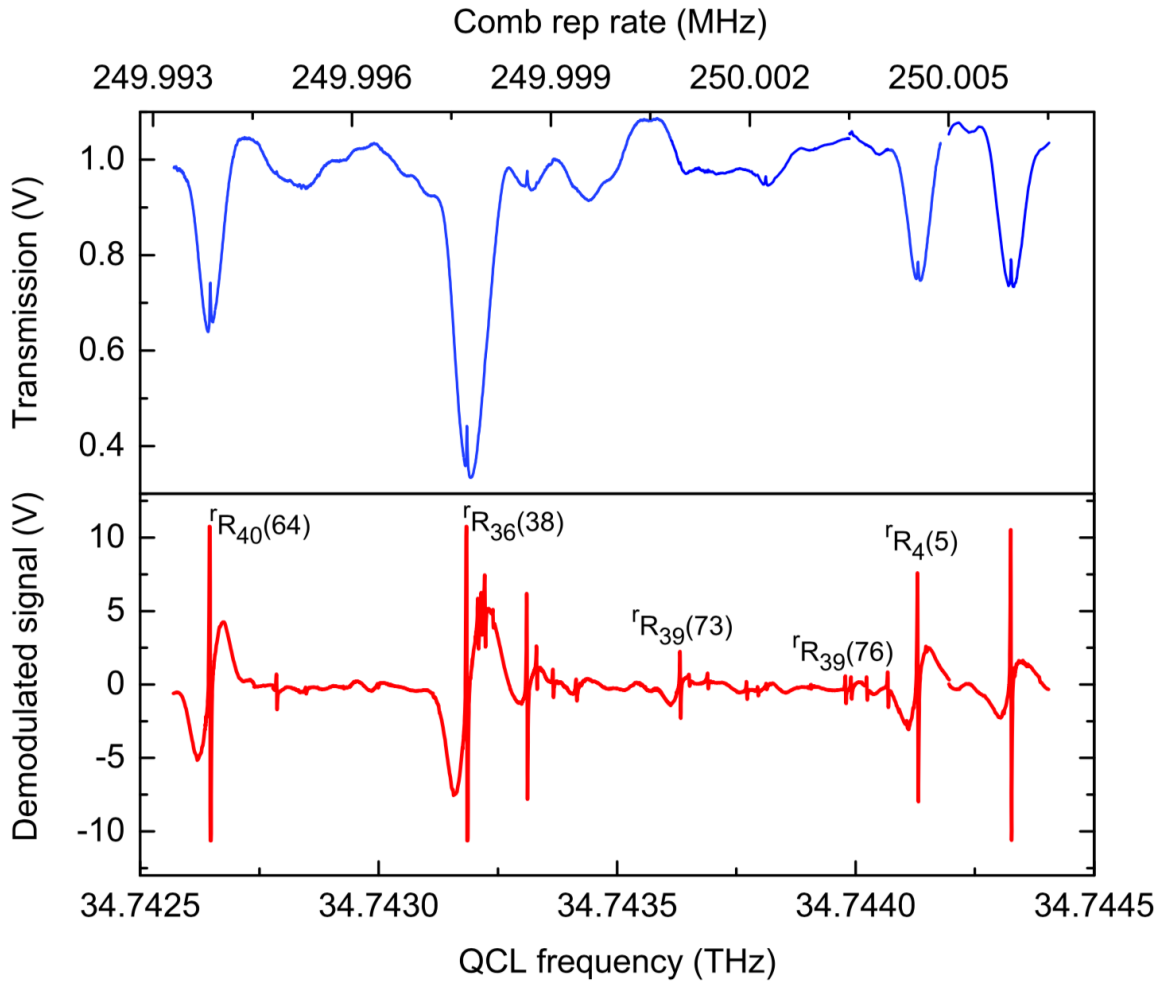
QCL linewidth

160 kHz at 1-s integration

Servo-loop BW: 250 kHz

A. Gambetta, et al., APL Phot. 3, 4 (2018)

Comb-assisted scanning



CHF_3 pressure
6.0(1) Pa

Pump beam power
5.0(3) mW

Pump beam radius
1.0(0) mm

Modulation parameters
 $f_m = 10$ kHz
 $a_m = 320$ kHz

Tens of saturated absorption lines in 2-GHz frequency span

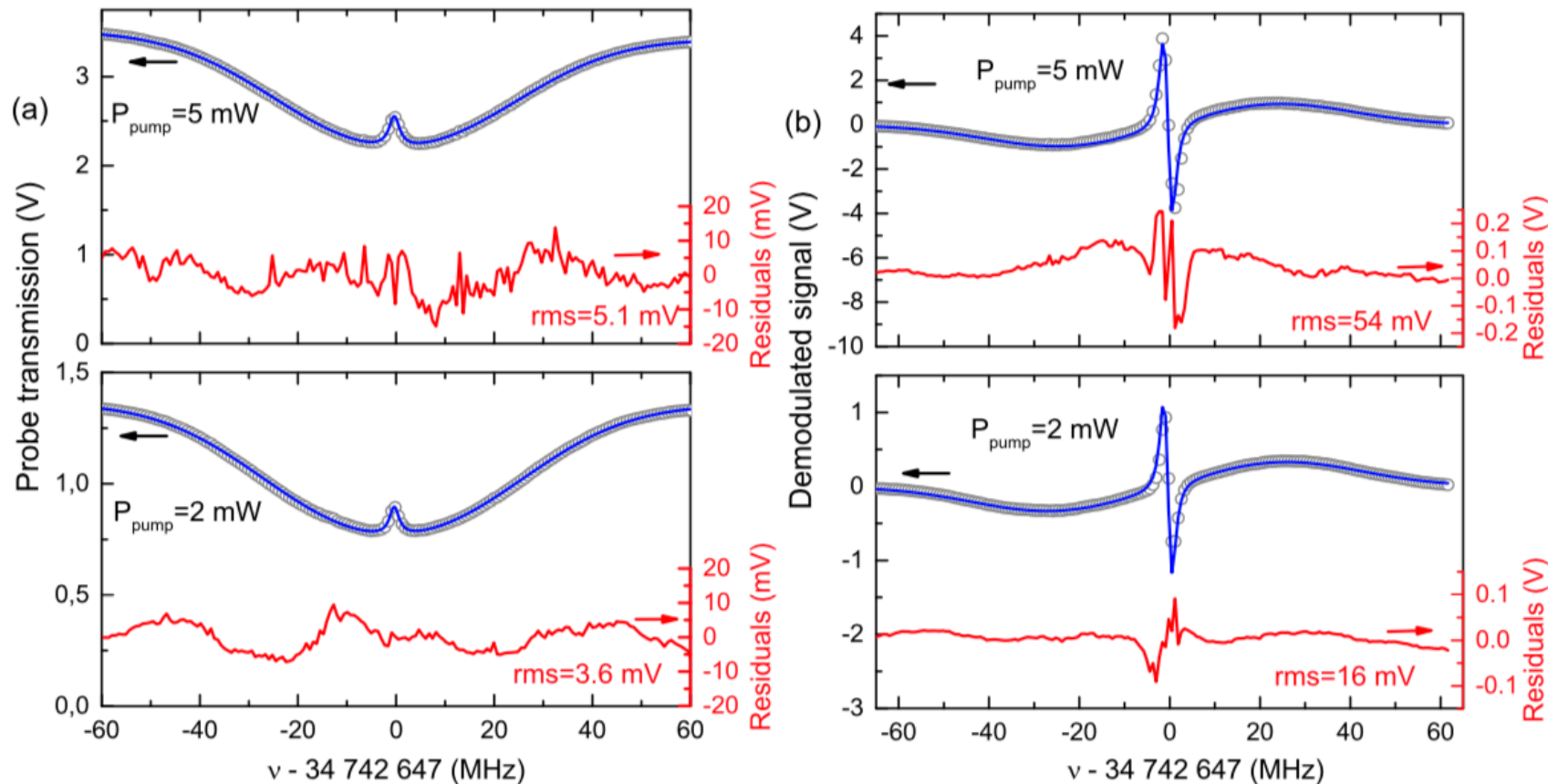
Lamb-dip linewidths and contrasts ranging from 1.5 to 2 MHz and from 1% to 20%

Highest SNR: 58 dB in 0.1 kHz integration bandwidth

Line	Frequency (MHz)	Wave number (cm ⁻¹)	Assignment		Obs. - Calc. (10 ⁻⁴ cm ⁻¹)	Line	Frequency (MHz)	Wave number (cm ⁻¹)	Assignment		Obs. - Calc. (10 ⁻⁴ cm ⁻¹)
			<i>v</i> ₅ band	<i>v</i> ₂ band					<i>v</i> ₅ band	<i>v</i> ₂ band	
1	34 742 647.0(1)	1158.889 961(3)	<i>r</i> R ₄₀ (64)		7.5	21	34 743 690.2(5)	1158.924 76(2)	<i>r</i> R ₄₀ (74)		-2.0
2	34 742 745(1)	1158.893 23(3)	—	—		22	34 743 771.4(5)	1158.927 48(2)	—	—	
3	34 742 786.4(5)	1158.894 61(2)	—	—		23	34 743 795(1)	1158.928 25(3)	—	—	
4	34 742 833(1)	1158.896 17(3)	<i>r</i> R ₃₉ (66)		4.1	24	34 743 813(1)	1158.928 86(3)		^q R ₃₆ (87)	0.4
5	34 742 847(1)	1158.896 63(3)	—	—		25	34 743 907(1)	1158.931 99(3)	—		
6	34 742 926(1)	1158.899 27(3)	<i>r</i> R ₄₁ (61)		5.5	26	34 743 978.9(5)	1158.934 39(2)	<i>r</i> R ₄₃ (78)		7.8
7	34 742 998(1)	1158.901 67(3)		^q R ₃₆ (79)	3.1				<i>r</i> R ₃₉ (76)		4.0
8	34 743 185.1(1)	1158.907 910(3)	<i>r</i> R ₃₆ (38)		0.3					^q R ₃₆ (86)	3.2
			<i>r</i> R ₃₇ (77)		4.9	27	34 743 991.0(5)	1158.934 79(2)		^q R ₃₆ (83)	0.7
			<i>r</i> R ₄₁ (75)		5.5	28	34 744 023.8(5)	1158.935 89(2)	—	—	
9	34 743 208.8(5)	1158.908 70(2)	—	—		29	34 744 067.9(5)	1158.937 36(2)		^q R ₃₆ (84)	3.7
10	34 743 216.1(5)	1158.908 94(2)	—	—						^q R ₃₆ (85)	5.7
11	34 743 223.2(3)	1158.909 18(1)	—	—		30	34 744 107(1)	1158.938 66(3)	<i>r</i> R ₃₇ (79)		3.5
12	34 743 240.2(5)	1158.909 75(2)	—	—		31	34 744 110(1)	1158.938 76(3)	—	—	
13	34 743 311.3(1)	1158.912 120(3)	—	—		32	34 744 130.6(1)	1158.939 449(3)	<i>r</i> R ₄ (5)		-1.4
14	34 743 331.6(3)	1158.912 80(1)	—	—		33	34 744 148(1)	1158.940 03(3)	<i>r</i> R ₃₈ (77)		-7.3
15	34 743 366.0(5)	1158.913 94(2)		^q R ₃₆ (80)	6.4	34	34 744 310(1)	1158.945 43(3)	<i>r</i> R ₃₉ (67)		7.1
16	34 743 415.0(5)	1158.915 58(2)	—	—					<i>r</i> R ₄₀ (46)		9.0
17	34 743 423(1)	1158.915 85(3)	—	—		35	34 744 326.0(1)	1158.945 967(3)	—	—	
18	34 743 632.5(3)	1158.922 83(1)	<i>r</i> R ₃₉ (73)		7.2	36	34 744 333(1)	1158.946 20(3)	—	—	
19	34 743 652(1)	1158.923 48(3)		^q R ₃₆ (81)	6.3						
20	34 743 676(1)	1158.924 29(3)	<i>r</i> R ₃₇ (78)		1.3						

The line center frequency is measured for 36 lines, with a best fractional precision of **2×10⁻⁹** in a single scan acquisition of 1000 s

Isolated $^1R_{40}$ (64) line

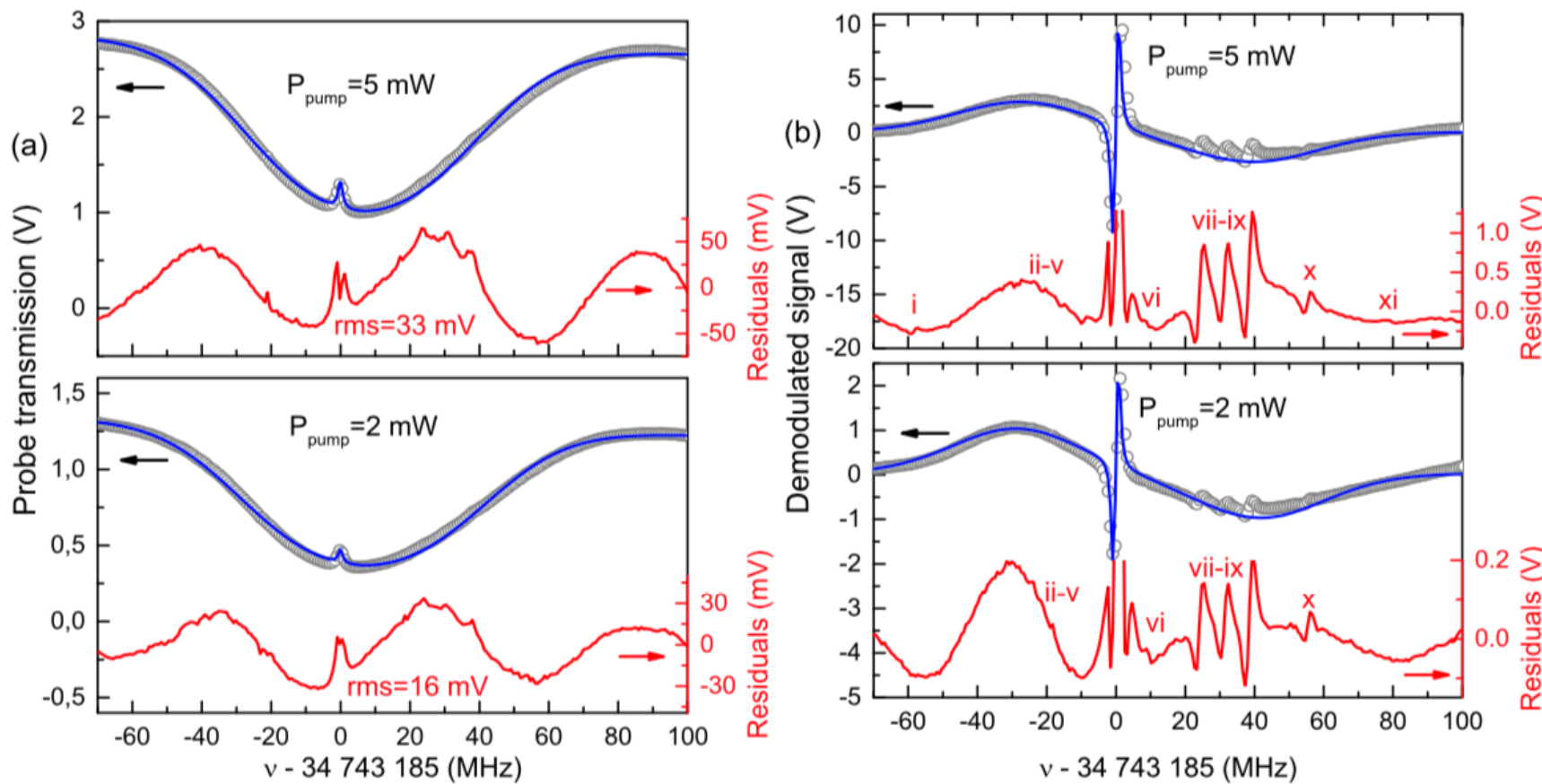


$$\alpha(\omega) = \alpha_0(\omega - \omega_{0,G}) \times \left\{ 1 - \left(1 - \frac{1}{\sqrt{1+S}} \right) N g_V(\omega - \omega_{0,V}) \right\}$$

$$Z_D(\omega) = (Z_0 + Z_1 \omega) \exp [-\alpha(\omega)L]$$

$$Z_{WM}(\omega) = (Z_0^{WM} + Z_1^{WM} \omega) + [S_{1,G}(\omega) + S_{1,V}(\omega)]$$

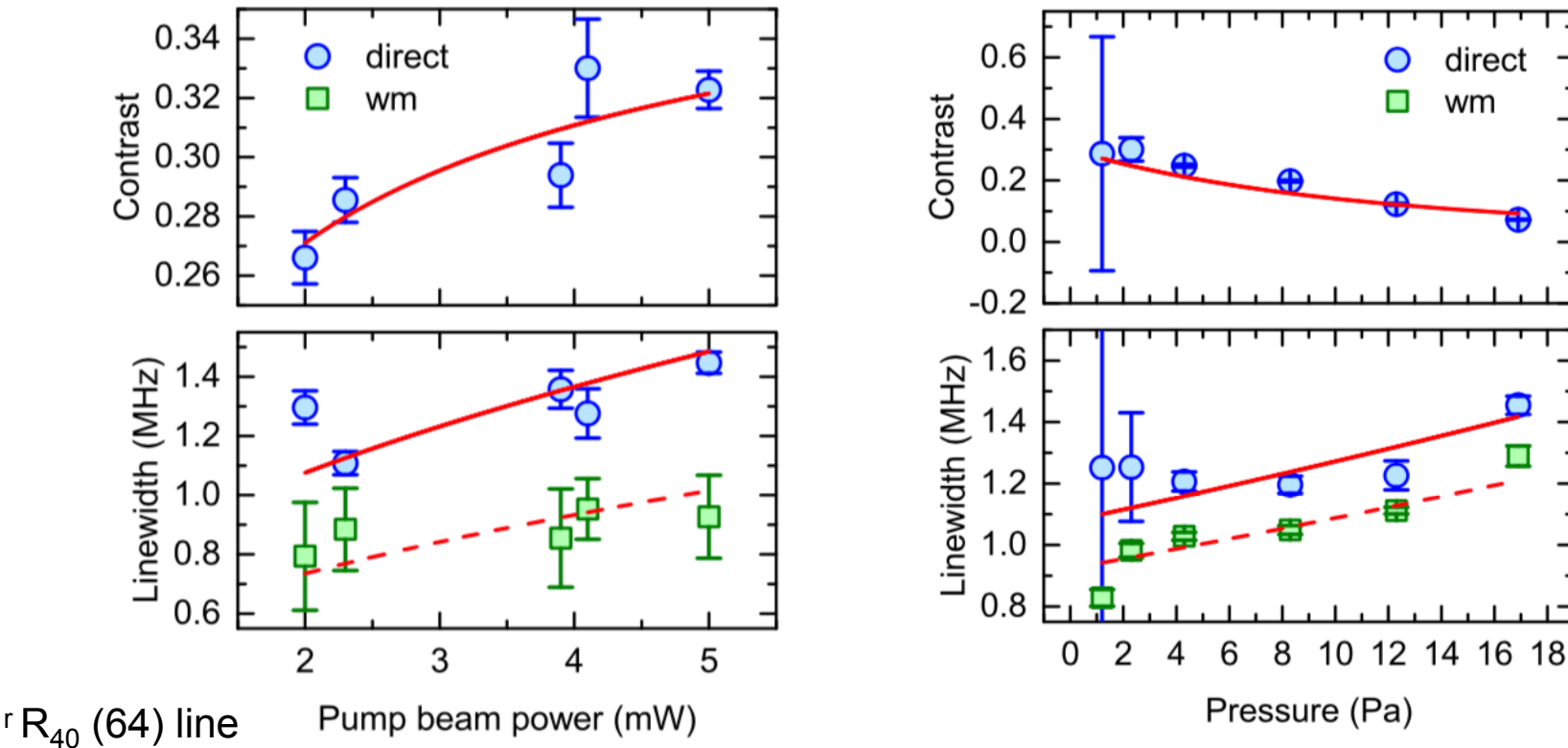
Multi $r R_{36}$ (38) line



$$\alpha(\omega) = \alpha_0(\omega - \omega_{0,G}) \times \left\{ 1 - \left(1 - \frac{1}{\sqrt{1+S}} \right) N g_V(\omega - \omega_{0,V}) \right\}$$

$$Z_D(\omega) = (Z_0 + Z_1 \omega) \exp [-\alpha(\omega)L]$$

$$Z_{WM}(\omega) = (Z_0^{WM} + Z_1^{WM} \omega) + [S_{1,G}(\omega) + S_{1,V}(\omega)]$$



${}^1\text{R}_{40}$ (64) line Pump beam power (mW)

	DS	WM
Saturation power, P_s , (mW)	0.3(1)	0.3(1)
Lorentzian linewidth, γ_0 , (MHz)	0.29(1)	0.20(1)
Rabi frequency, Ω_0 , (MHz)	0.7(2)	0.8(2)
Pressure broadening, B_p , (MHz/Pa)	0.016(2)	0.013(2)

Transition
electric dipole moment
 $(7 \pm 1) \cdot 10^{-31} \text{ C m}$
 $(0.22 \pm 0.04) \text{ Debye}$

- ✓ Direct phase-locking of a QCL at 8.6 μm to a mid-IR frequency comb
 - ✓ QCL-line narrowing down to 160-kHz (FWHM)
- ✓ High-precision sub-Doppler spectroscopy of CF_3H at 8.6 μm
 - ✓ 0.3-kHz (10^{-11}) frequency axis accuracy
 - ✓ 150-MHz/min tuning speed
 - ✓ Best SNR 59 dB at 100 Hz integration bandwidth
 - ✓ Transition electric dipole moment measurement

Future perspectives

Non-linear spectroscopic of cold CF_3H (100-150 K) at 8.6 μm

- ✓ Two-photon spectroscopy
- ✓ Hyperfine structure measurement

Thank you for attention



N. Coluccelli



A. Gambetta



T. T. Fernandez



Y. Wang



E. Vicentini



P. Laporta



G. Galzerano



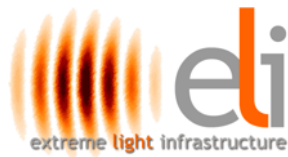
UNIVERSITÀ DEGLI STUDI
DELLA CAMPANIA
LUIGI VANVITELLI

E. Fasci
L. Gianfrani
A. Castrillo

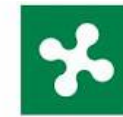


INO-CNR
ISTITUTO
NAZIONALE DI
OTTICA

V. Di Sarno
L. Santamaria
P. De Natale
P. Maddaloni

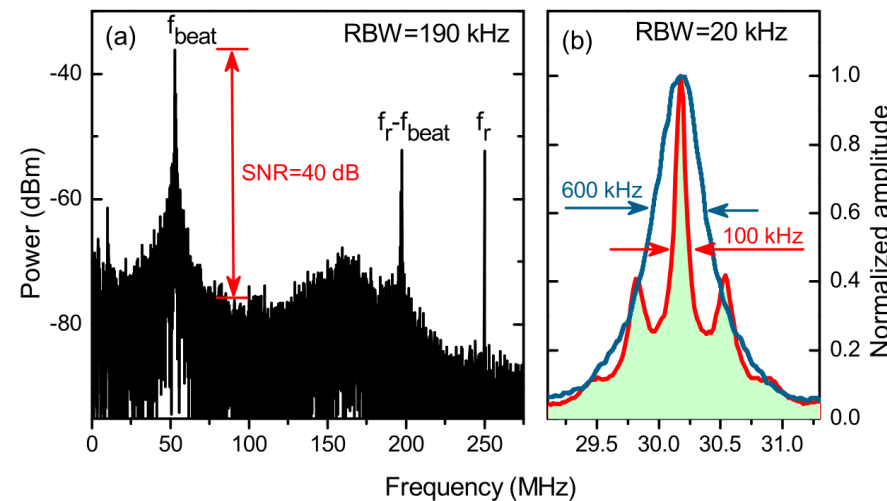


MINISTERO DELL'ISTRUZIONE,
DELL'UNIVERSITÀ E DELLA RICERCA



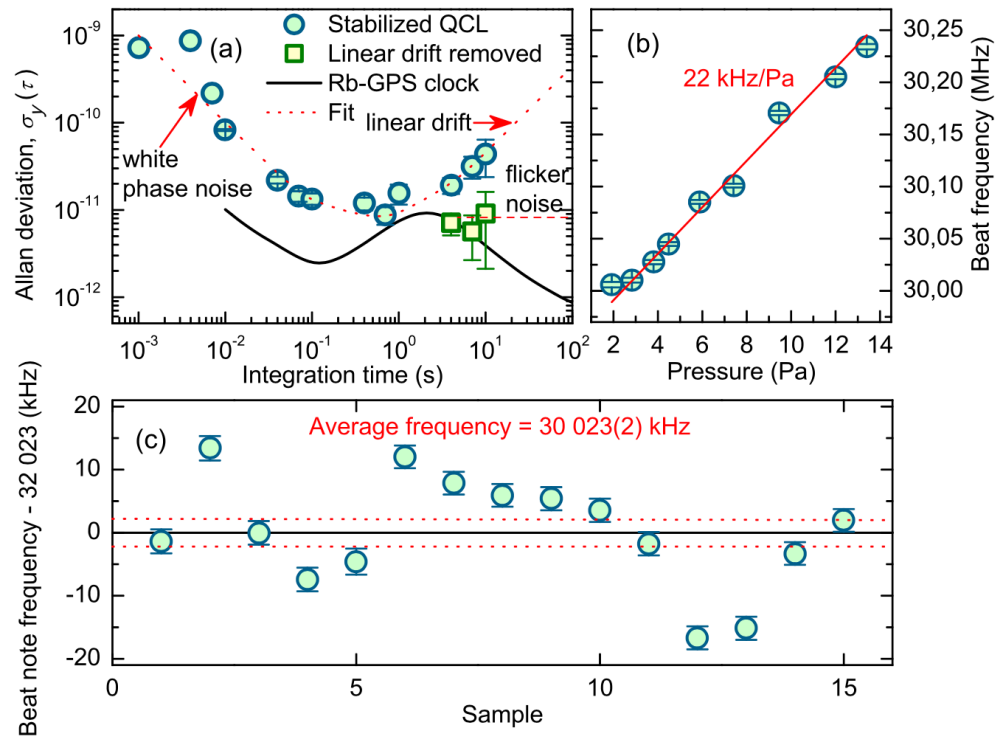
RegioneLombardia

Frequency stabilization against saturated CF_3H absorption line



Uncertainty budget

Parameter	Coefficient	Type B Uncertainty (kHz)
CHF_3 pressure, p_{CHF_3}	$22(1) \text{ kHz/Pa}$	0.75
Gas cell leakage, p_{leak}	$38(2) \text{ kHz/Pa}$	1.5
Laser power, P_{QCL}	45 kHz/mW	0.2
Modulation frequency, f_m	100 Hz/kHz	Negligible
Modulation depth, a_m	16 kHz/MHz	Negligible
Electronic offset	0.3 kHz/mV	0.2
Etalon/interference effects		0.5
Rb-GPS clock		0.04
Total type B uncertainty		$1.8 (5 \cdot 10^{-11})$



R_{36} (38) line center frequency
34 743 124 881(2) kHz
 Fractional accuracy 6×10^{-11}

A. Gambetta et al, Opt. Lett. **42**, 1911-1914, 2017